Ecological Indicators 160 (2024) 111921

Contents lists available at ScienceDirect

Ecological Indicators

journal homepage: www.elsevier.com/locate/ecolind

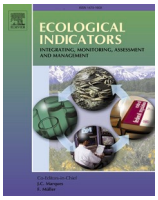

Influence of climate zone shifts on forest ecosystems in northeastern United States and maritime Canada

Samuel Roy [a], Xinyuan Wei [a,b], Aaron Weiskittel [a,b,*], Daniel J. Hayes [a,b], Peter Nelson [c], Alexandra R. Contosta [d]

[a] School of Forest Resources, University of Maine, Orono, ME 04469, USA
[b] Center for Research on Sustainable Forests, University of Maine, Orono, ME 04469, USA
[c] Schoodic Institute at Acadia National Park, Winter Harbor, ME 04693, USA
[d] Earth Systems Research Center, University of New Hampshire, Durham, NH 03824, USA

ARTICLE INFO

Keywords:
Climate change
Climate zone
Delineation
Forest ecosystem
Maritime Canada
Northeastern United States
Prediction

ABSTRACT

Climate zones play a significant role in shaping the forest ecosystems located within them by influencing multiple ecological processes, including growth, disturbances, and species interactions. Therefore, delineation of current and future climate zones is essential to establish a framework for understanding and predicting shifts in forest ecosystems. In this study, we developed and applied an efficient approach to delineate regional climate zones in the northeastern United States and maritime Canada, aiming to characterize potential shifts in climate zones and discuss associated changes in forest ecosystems. The approach comprised five steps: climate data dimensionality reduction, sampling scenario design, cluster generation, climate zone delineation, and zone shift prediction. The climate zones in the study area were delineated into four different orders, with increasing subzone resolutions of 3, 9, 15, and 21. Furthermore, projected climate normals under Shared Socioeconomic Pathways 4.5 and 8.5 scenarios were used to predict the shifts in climate zones until 2100. Our findings indicate that climate zones characterized by higher temperatures and lower precipitation are expected to become more prevalent, potentially becoming the dominant climate condition across the entire region. Thes changes are likely to alter regional forest composition, structure, and productivity. In short, such shifts in climate underscore the significant impact of environmental change on forest ecosystem dynamics and carbon sequestration potential.

1. Introduction

The characteristics of forest ecosystems are largely determined by their climate conditions, which strongly control the availability of energy and water (Gounand et al., 2020; Grimm et al., 2013). Climate zones are geographical areas with similar prevailing weather conditions, which are defined by a combination of variables such as temperature, precipitation, atmospheric pressure, and humidity (Geletič et al., 2019; Liu and Shi, 2020). Thus, identifying the unique characteristics of different climate zones is essential for investigating how forest ecosystems respond to climate change, how tree species distributions shift in response to changing climate conditions, and what management strategies are needed to ensure the long-term sustainability of forest ecosystems (Gilliam, 2016; Walther et al., 2002). For example, studying the relationship between climate and forest ecosystem productivity is crucial for comprehending how variations in temperature and precipitation affect forest production (Zhao et al., 2023a; Zhao et al., 2023b) and carbon sequestration capabilities (Chapin et al., 2006; Wei et al., 2024). Additionally, analyzing the distribution and abundance of tree species across various climate zones is required to identify areas of high biodiversity and prioritize management or conservation efforts (Araújo et al., 2011; Hoffmann et al., 2015). Therefore, delineating climate zones is a crucial step in forest ecosystem research as it provides a framework for understanding the interactions between ecosystems and their environment (von Buttlar et al., 2018). Ultimately, this understanding informs management and conservation strategies that are important for maintaining the health and resilience of ecosystems at various scales, from regional to global.

The delineation of climate zones, ranging from regional to global scales (Demuzere et al., 2019; Rosentreter et al., 2020), is necessary for understanding and predicting forest ecosystems, including ecological processes, structure diversity, and vegetation species shifts (Manes et al.,

* Corresponding author.
E-mail address: aaron.weiskittel@maine.edu (A. Weiskittel).

https://doi.org/10.1016/j.ecolind.2024.111921
Received 6 December 2023; Received in revised form 29 February 2024; Accepted 19 March 2024
Available online 25 March 2024

2021; Rahbek et al., 2019). At the regional scale, climate zones can help identify the key environmental factors that shape tree species diversity, reveal how different species are distributed across these zones, and provide insight into how they might respond to climate change (Freeman et al., 2021; Taheri et al., 2021). At the continental scale, climate zones are useful in identifying forest regions of high conservation value and biodiversity hotspots (Habel et al., 2019; Trew and Maclean, 2021) along with understanding and predicting how climate affects the broad-scale distributions of different forest ecosystems (Laganiere et al., 2010). At the global scale, climate zones are important for understanding the distribution, diversity, and productivity of different biomes across the world, as well as for developing effective policies and strategies for maintaining and conserving global ecosystems in the face of different environmental challenges (Gardner et al., 2020; Zheng et al., 2016).

Climate zones are typically defined by grouping regions with similar long-term weather conditions based on statistical clustering of long-term weather data. The clustering approach simplifies the analysis of large multivariate climate datasets into a smaller number of discrete values (Iyigun et al., 2013). Numerous methods have been developed and applied to delineate climate zones. For example, the Köppen climate classification system is a prevalent method for delineating homogeneous climate zones at regional to global scales, using temperature and precipitation as essential meteorological elements for categorization (Beck et al., 2018; de Sá Júnior et al., 2012; Demuzere et al., 2019). Briggs and Lemin (1992) delineated climate zones in Maine, USA, by employing historical observations from 63 weather stations and using a cluster analysis methodology. Bunkers et al. (1996) used an objective modification approach and long-term climate records obtained from 147 weather stations in the U.S. Northern Plains to improve the borders of existing identified climate zones. Rhee et al. (2008) obtained weather information from both *in-situ* observations and remote sensing, then applied a consensus clustering method to delineate climate zones in the Carolinas region of the USA. Nusrat et al. (2020) developed a machine learning approach that used both remotely-sensed and model-estimated weather data to delineate climate zones within river basins of Pakistan. Mahmud et al. (2022) employed several clustering algorithms, such as hierarchical clustering, partitioning around medoids, and *K*-means, to identify climate zones in Bangladesh using weather station data. These approaches differ in their selection of climate variables, input data format (e.g., point data, surface data), methods of cluster generation, and statistical grouping techniques. Consequently, identifying the most suitable climate data and employing the optimal methodology for delineating climate zones within a study region presents a challenge, as the most effective approach is contingent upon the characteristics of climate.

In the past three decades, climate monitoring systems and interpolation methods have undergone significant advancements that enable the recording of numerous climate variables at high frequencies and fine spatial resolutions (Atzberger, 2013; Bramer et al., 2018). However, selecting the appropriate climate variables and the approach to effectively capture and represent all climate conditions across a given study area remains a challenge. Climate is the primary driving factor for the diversity of forest ecosystems in the northeastern United States and maritime Canada, which covers numerous transitional forest ecosystems (Evans and Brown, 2017). Therefore, delineating climate zones in this region and projecting their plausible futures are required to study and predict forest ecosystem shifts (Samal et al., 2017). In this study, we developed an efficient approach for delineating regional climate zones under projected climate change scenarios in this region and exploring potential forest ecosystem changes.

2. Materials and methods

2.1. Study area and climate data

The study area encompasses the northeastern United States and adjacent maritime Canada (Fig. 1), covering an area exceeding 533,000 km^2 and including all or portions of seven U.S. states (New York, Connecticut, Rhode Island, Massachusetts, Vermont, New Hampshire, and Maine) and four Canadian provinces (Quebec, New Brunswick, Nova Scotia, and Prince Edward Island). The majority of this region is situated at the polar front, which is a dynamic boundary zone between the moist subtropical air masses of the lower latitudes and the cold sub-polar maritime air masses to the north (Ricketts, 1999). Forest ecosystems in this region experience a wide range of average annual temperatures, varying from −4°C to 15 °C, and the average annual precipitation levels ranging from 500 to 1500 mm (NCEI, 2023). The spatiotemporal distribution of precipitation in this region is highly variable, with the summer months typically experiencing the highest levels while the winter months tend to be drier (NCEI, 2023). This climate variability can be attributed to several factors, including the complex topography, proximity to the coast or the Great Lakes, and their interactions (Oldfather et al., 2020). In addition, recent climate observations indicate that the region is experiencing a rapid warming trend and an increase in both the frequency and intensity of extreme precipitation events (Fernandez et al., 2020; Leduc et al., 2019).

The climate information provided by the ClimateNA database (Wang et al., 2016) was used to delineate climate zones in the study area. ClimateNA provides high spatial resolution and gridded climate information (1 × 1 km) for the entire North American continent, and it includes more than 200 climate variables such as the mean annual temperature, mean annual precipitation, and annual heat-moisture index (Mahony et al., 2022; Wang et al., 2016). ClimateNA uses a combination of weather station observations, climate model output, remote sensing images, and digital elevation models to calculate monthly, seasonal, and annual climate variables for any specific location (Wang et al., 2016). In addition, it provides projected climate predictions representing future Shared Socioeconomic Pathways 4.5 (SSP2-4.5) and 8.5 (SSP5-8.5) scenarios by using a 13-model ensemble and an 8-model subset from the Coupled Model Intercomparison Project Phase 6 (CMIP6) archives (Wang et al., 2016). Plausible shifts of current climate zones were projected using predicted climate information under scenarios SSP2-4.5 and SSP5-8.5. Therefore, four sets of climate normals including historical records and projected futures were used, spanning the time periods of 1961–1990, 2011–2040, 2041—2070, and 2071–2100. The gridded climate data extracted from ClimateNA was comprised of 533,768 1 × 1 km cells for our study area.

According to the analysis of ClimateNA data, the northeastern United States and adjacent maritime Canada are anticipated to experience significant climatic alterations in the future (Table 1). During the reference period of 1961–1990, the mean annual temperature was recorded at 5.5 ± 2.1 °C. However, projections under the SSP2-4.5 and SSP5-8.5 scenarios indicate an escalation to 9.1 ± 2.0 °C and 11.5 ± 1.8 °C, respectively, by the 2071–2100 timeframe. In parallel, both the mean warmest month and mean summer temperatures are predicted to experience moderate increases. Winters are projected to become warmer, as the mean winter temperature is anticipated to increase from −7.4 ± 2.9 °C to −3.2 ± 2.6 °C under the SSP2-4.5 scenario, and further to −0.8 ± 2.3 °C under the SSP5-8.5 scenario. Additionally, annual precipitation is projected to increase, reaching 1206 ± 145 mm and 1248 ± 147 mm under the SSP2-4.5 and SSP5-8.5 scenarios, respectively, within the 2071–2100 interval. Furthermore, an increase in frost-free days is anticipated, accompanied by an increase in relative humidity. The annual and summer heat moisture indices are projected to exhibit an upward trajectory, signifying a transition towards warmer and more humid conditions within the region.

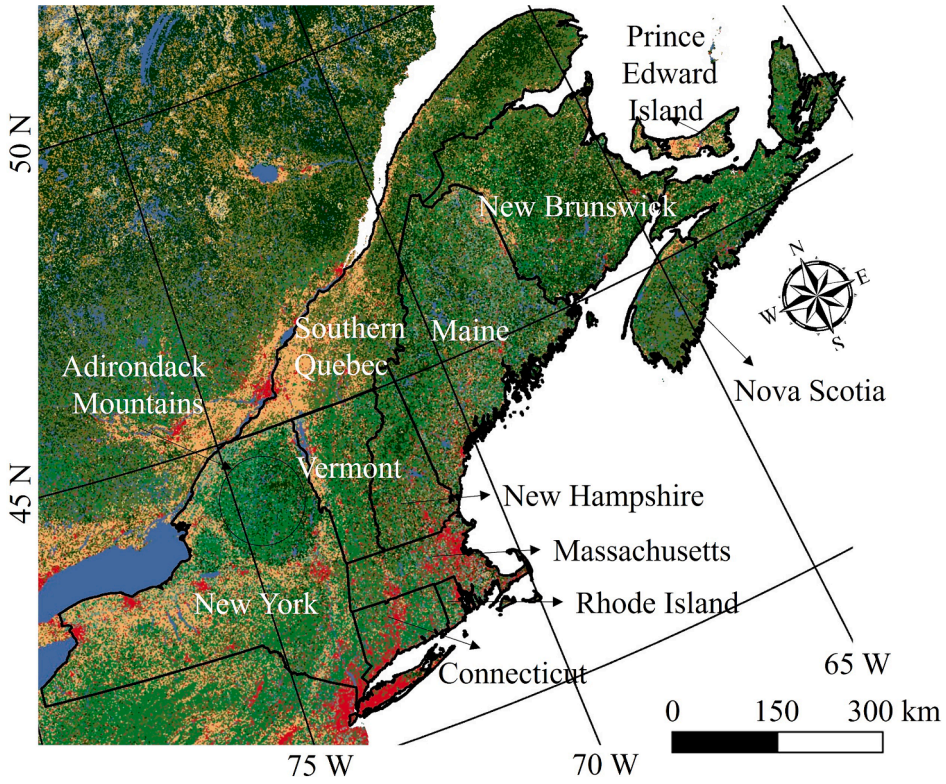

Fig. 1. The study region is the northeastern United States and adjacent maritime Canada.

Table 1
A summary of key climate variables (mean ± one standard deviation) for the northeastern United States and adjacent maritime Canada using the ClimateNA data.

Climate variable	1961–1990	SSP2-4.5			SSP5-8.5		
		2011–2040	2041–2070	2071–2100	2011–2040	2041–2070	2071–2100
Annual temperature (°C)	5.5 ± 2.1	7.3 ± 2.1	8.4 ± 2.0	9.1 ± 2.0	7.5 ± 2.0	9.4 ± 2.0	11.5 ± 1.8
Warmest month temperature	18.9 ± 1.7	20.7 ± 1.7	21.8 ± 1.7	22.4 ± 1.7	20.8 ± 1.7	22.7 ± 1.7	25.0 ± 1.7
Summer temperature	17.5 ± 1.8	19.3 ± 1.8	20.4 ± 1.8	21.0 ± 1.8	19.5 ± 1.8	21.3 ± 1.8	23.5 ± 1.8
Winter temperature	−7.4 ± 2.9	−5.4 ± 2.8	−4.0 ± 2.7	−3.2 ± 2.6	−5.2 ± 2.7	−3.0 ± 2.5	−0.8 ± 2.3
Coldest month temperature	−8.6 ± 3.1	−6.6 ± 3.0	−5.2 ± 2.8	−4.3 ± 2.7	−6.6 ± 2.9	−4.2 ± 2.7	−1.8 ± 2.4
Annual precipitation (mm)	1106 ± 135	1168 ± 139	1192 ± 144	1206 ± 145	1159 ± 140	1208 ± 143	1248 ± 147
Summer precipitation	481 ± 43	502 ± 45	506 ± 46	510 ± 46	502 ± 45	512 ± 46	514 ± 46
Winter precipitation	257 ± 63	279 ± 66	286 ± 67	296 ± 68	272 ± 66	294 ± 67	315 ± 71
Number of frost free days	160 ± 20	178 ± 21	189 ± 21	197 ± 22	179 ± 20.5	200 ± 21	223 ± 22
Relative humidity (%)	61.9 ± 4.3	63.0 ± 4.3	63.8 ± 4.3	64.2 ± 4.3	63.2 ± 4.3	64.5 ± 4.4	66.0 ± 4.3
Annual heat moisture index	14.2 ± 2.7	15.0 ± 2.7	15.7 ± 2.8	16.1 ± 2.8	15.3 ± 2.7	16.3 ± 2.8	17.5 ± 2.9
Summer heat moisture index	39.6 ± 5.4	41.6 ± 5.6	43.5 ± 5.9	44.4 ± 5.9	41.9 ± 5.7	44.9 ± 6.0	49.1 ± 6.3

2.2. Climate zones delineation and prediction

The approach comprised five steps: climate data dimensionality reduction, sampling scenario design, cluster generation, climate zone delineation, and zone shift prediction. Initially, Principal Component Analysis (PCA) was applied to reduce the dimensionality of 75 climate variables and address multicollinearity, identifying key components that capture the majority of variance in climate data. In the sampling scenario design, various sample sizes were tested against criteria such as computational efficiency and representativeness to determine the optimal strategy for effectively delineating climate zones. Cluster generation was realized through agglomerative hierarchical clustering, using principal components to group similar samples and minimize within-cluster variance based on Euclidean distance. Climate zone delineation then categorized the remaining cells into distinct clusters using the *K*-nearest neighbor algorithm, leveraging its non-parametric nature for spatial data classification, informed by the clusters generated in the previous step. Finally, zone shift prediction employed predictive models, utilizing historical and predicted climate normals based on climate models and emission scenarios, to forecast future climate zone shifts and identify regions likely to experience obvious climate changes. This comprehensive methodology ensures a robust analysis of climate zone dynamics and their potential shifts.

2.2.1. Climate dimensionality reduction

In this study, we selected monthly normals for 75 climate variables, which describe temperature and precipitation from various perspectives, such as monthly mean temperature and total precipitation, to delineate the current climate zones (Table S1); however, numerous variables are highly correlated and may result in the overfitting of our delineation. Therefore, a PCA was performed to identify highly correlated climate variables, investigate the relative contribution of each variable in maximizing the variance in climate data among different regions, and reduce the dimensionality of the data set (Daffertshofer et al., 2004). Because these climate variables are in different units, a correlation matrix was used in performing PCA. The PCA results suggest

that loadings of multiple monthly climate variables are similarly distributed, and they are correlated to seasonal patterns. Consequently, we recalculated the mean, minimum, and maximum temperatures, as well as total precipitation for each season, replacing their monthly values. Eventually, 39 climate variables were used to delineate climate zones for our study area (*Table S2*). In addition, 96 % of the total variance in the climate data can be accounted for by the first five principal components (PCs). The cumulative explained variance by the first PC is 63.5 %, which is primarily influenced by temperature-related seasonal and annual averages, frost-free periods, and degree-day variables (Fig. 2). The second PC has higher magnitude loadings for non-summer precipitation variables, relative humidity, moisture indices, and continental climate effects. It has a cumulative explained variance of 83.4 %. The third PC has a cumulative explained variance of 91.6 %, which has higher magnitude loadings for non-winter precipitation variables, evaporation, and relative humidity. The fourth PC (cumulative explained variance = 94.4 %) is characterized by higher magnitude loadings for solar radiation, relative humidity, precipitation, and moisture deficit, while the fifth PC (cumulative explained variance = 96.7 %) is dominated by solar radiation with little contribution from other variables.

2.2.2. Sampling scenario design

Given the computational challenges of directly delineating climate zones from the large number of cells in our study area (533,768 1 × 1 km^2 grids), we input a sample of cells to an agglomerative algorithm to generate clusters. Subsequently, we employed a *K*-nearest neighbor classification method to categorize the remaining cells. Initially, various sampling scenarios were tested to identify the optimal sampling strategy. Instead of using a statistical index, such as maximum distance thresholds, to discretize an arbitrary number of climate zones, a maximum number of climate zones was predefined. The National Centers for Environmental Information (NCEI, 2023) identified 25 climate divisions within the northeastern United States and Gullett and Skinner (1992) characterized three distinct climate regions in maritime Canada. As the climate divisions are also demarcated by state boundaries, we integrated those with similar characteristics that spanned across multiple states, ultimately identifying 20 climate regions within the northeastern United States. Consequently, the maximum number of climate zones in the study area was determined to be 23.

Formann (1984) suggested that to obtain reliable cluster results, it requires more than $5 \times 2^{\delta}$ samples across the study area, where δ is the number of objective variables. In addition, Qiu and Joe (2009) determined that the required number of samples is no less than $10 \times \delta \times \xi$, where ξ is the number of target clusters. In this study, the objective variables are the five PCs, and the maximum number of clusters (climate zones) is 23, making the minimum required sample size 160 or 1150 based on the two approaches. According to these requirements, we designed eight sample scenarios, which increased the number of samples from 3,000 to 10,000 with a 1,000 increment. For each sample size, the sample cells' locations were randomly generated on the landscape and this step was repeated 50 times. So, 400 (8 sample size × 50 random sample scenarios) tests were performed for each predefined number of clusters (climate zones, ranging from 2 to 23 for increments of one).

2.2.3. Cluster generation

Ward's method, an agglomerative hierarchical clustering algorithm (Murtagh and Legendre, 2014; Szekely and Rizzo, 2005), was used to group similar samples into clusters based on the five PCs. This method groups similar sample cells together into clusters and minimizes the within-cluster variance based on the Euclidean distance between cluster centers and sample cells. Therefore, this approach produces compact and spherical clusters of roughly equal size (Szekely and Rizzo, 2005). After agglomerating these 5,000 samples to clusters, the silhouette score was used to measure how similar a sample is to its own cluster (cohesion) compared to other clusters (separation) (Shahapure and Nicholas, 2020). The silhouette score was calculated for each sample and ranges between −1 and + 1. A higher score indicates that a sample is well-matched to its own cluster and poorly matched to neighboring clusters, while a lower score indicates the opposite. A score of 0 indicates that the sample cell is on the boundary between two clusters.

For each sampling scenario, the Ward's hierarchical clustering method was applied to generate clusters, then the silhouette score was calculated to assess its performance. The results indicate that the sampling scenario of 5,000 samples is the optimal choice and increasing the sample size did not provide significant improvement in the silhouette score. The 50 random sampling scenarios indicate that the sample locations have no obvious influence on silhouette score (Fig. 3a). Therefore, we found that a random selection of samples from the landscape can reliably identify and delineate well-defined climate zones. This is because adequate samples (5,000) ensure that the delineation of climate zones is not influenced by the random positioning of sample cells (Dalmaijer et al., 2022). Furthermore, we found that the silhouette score significantly decreased when the number of climate zones increased

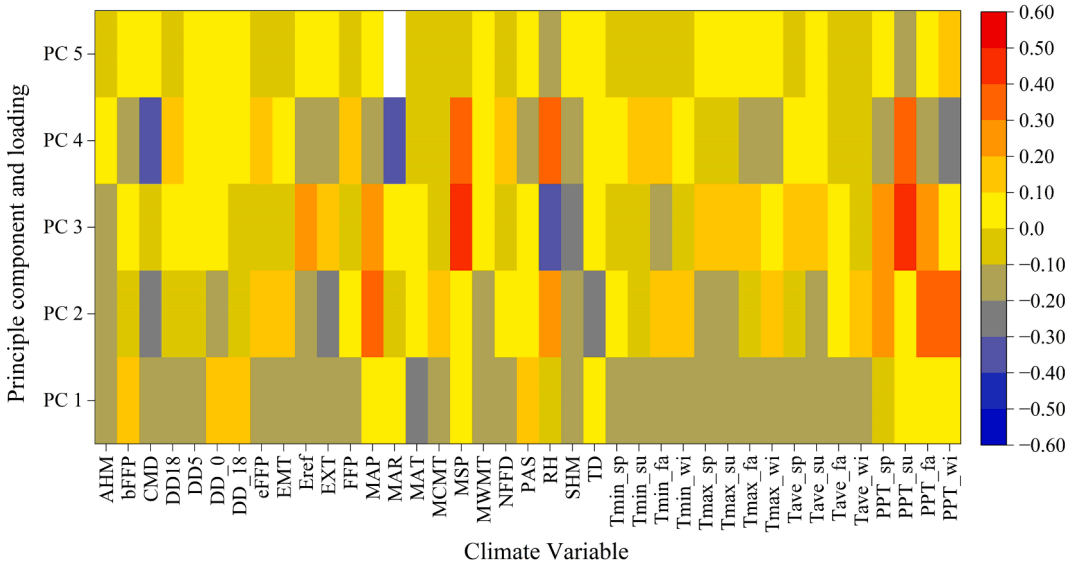

Fig. 2. The 39 climate variables identified by the Principal Component Analysis (PCA) and their loadings. (The detail of each climate variable is in the supporting information Table S1.).

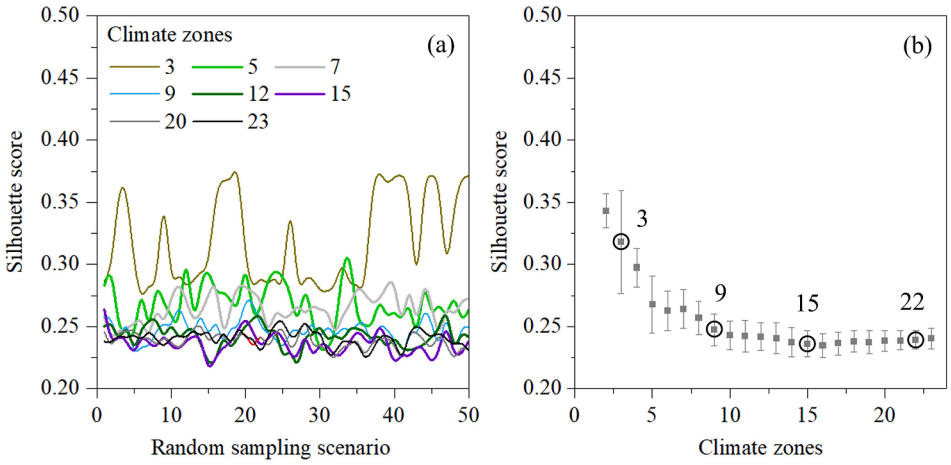

Fig. 3. The silhouette score for each of 50 random sample scenarios when the number of climate zones for the study area was set at 3, 5, 7, 9, 12, 15, 20, and 23 (a), and the average silhouette score, along with its one standard deviation (from the 50 sampling methods), as the number of climate zones increased incrementally from 2 to 23 (b).

from 2 to 10 before stabilizing (Fig. 3b). In this study, we decided to delineate the study region into 3 (silhouette score = 0.377), 9 (0.247), 15 (0.255), and 21 (0.249) climate zones, which adequately represented the various levels of silhouette scores.

2.2.4. Climate zone delineation

To categorize the remaining cells (excluding the 5,000 samples) into distinct clusters (climate zones), the *K*-nearest neighbor classification algorithm was used, with the PCs serving as objective variables. The *K*-nearest neighbor algorithm is a non-parametric, supervised learning classifier that relies on proximity to classify individual cells (Chomboon et al., 2015). In addition, the clusters generated by the 5,000 samples were used as target variables to train this algorithm. Furthermore, each climate zone was identified in the northeastern United States and maritime Canada. In this study, the delineating processes were repeated for 3, 9, 15, and 21 climate zones. Because the same training data were used, the four orders of climate zones have a nested structure. For example, three primary climate zones were subdivided to produce nine second order zones.

2.2.5. Zone shift prediction

We delineated climate zones for four time periods by using historical climate normals in the period of 1961–1990 and predicted climate normals for 2011–2040, 2041–2070, and 2071–2100. Because this delineation approach could not generate new clusters (climate zones), we therefore applied the local outlier factor algorithm (Mishra and Chawla, 2019; Xu et al., 2022) to identify regions projected to undergo significant climate change. The local outlier factor algorithm identifies anomalous cells by measuring the local deviation of a cell with respect to its neighbor cells using the same five PCs. When the predicted climate normals for given cells are identified as outliers from their current climate zone, and they exhibit similar predicted climate conditions, these cells are reclassified into a new climate zone nested within the previous one.

This approach is sensitive to automatically identifying cells with projected changes in climate; however, the constraint to generate new climate zones is a manipulated condition. In this study, we employed a contamination parameter of 0.1 % to define the proportion of outliers in each climate zone. This means that the climate conditions in 0.1 % of a climate zone are assumed to have changed significantly and are no longer considered part of its current climate zone. While the low contamination parameter value increased the computational load, it reduced the likelihood of excessive outlier detection (Fujisawa and Eguchi, 2008), resulting in the identification of more cells as outliers.

2.3. Forest matrix

This study assessed the impact of climate zone shifts on various aspects of forest ecosystems, including forest type, age, structure, and aboveground biomass (AGB). We first analyzed the relationship between climate zones and forest types across our study area, using forest type data from the National Land Cover Database (NLCD) (Yang et al., 2018). We then examined the influence of climate on forest age by comparing forest age data (Besnard et al., 2021) with the climate zones. This analysis helped us understand the role of climate in shaping forest age distribution. Furthermore, we investigated how climate zones affect forest structure by analyzing their correlation with canopy height data (Potapov et al., 2021). Finally, we explored the impact of climate zone shifts on the carbon storage capacity of forests by comparing the climate zones with AGB data provided by Spawn and Gibbs (2020). Furthermore, recognizing that human activities such as harvesting and reforestation can significantly impact forest ecosystems (Danneyrolles et al., 2019), we incorporated US Forest Service, Forest Inventory and Analysis (FIA) data into our study. To minimize the influence of human activities on our findings, we specifically selected forest plots with stand ages exceeding 100 years. This selection ensures that the observed changes and patterns in forest ecosystems are predominantly attributable to climatic factors, rather than recent human interventions.

3. Results

3.1. Current climate zones

Our proposed approach was used to delineate the climate zones in the northeastern United States and maritime Canada, resulting in the delineation of four orders of climate zones with increasing subzone resolutions of 3, 9, 15, and 21. For the first-order of climate zones, the climate zone CZ0 covers 40 % of the region and dominates southern New England, New York, and coastal Maine (Fig. 3a). CZ0 is characterized by its high average annual temperature (Fig. 4a) and has the largest number of frost-free days compared to the other two climate zones (Fig. 4c). Climate zone CZ1 is 46 % of the study area and encompasses the Adirondack Mountains, Vermont, northern New Hampshire, northern Maine, New Brunswick, and southern Quebec (Fig. 3a), and it exhibits the lowest mean annual temperature (Fig. 4a) and the fewest frost-free days (Fig. 4c) among the climate zones. However, CZ0 and CZ1 have similar mean annual precipitation and mean annual relative humidity (Fig. 4b and 4d). On the other hand, climate zone CZ2, which covers the least area of 14 %, includes Nova Scotia, and Prince Edward Island

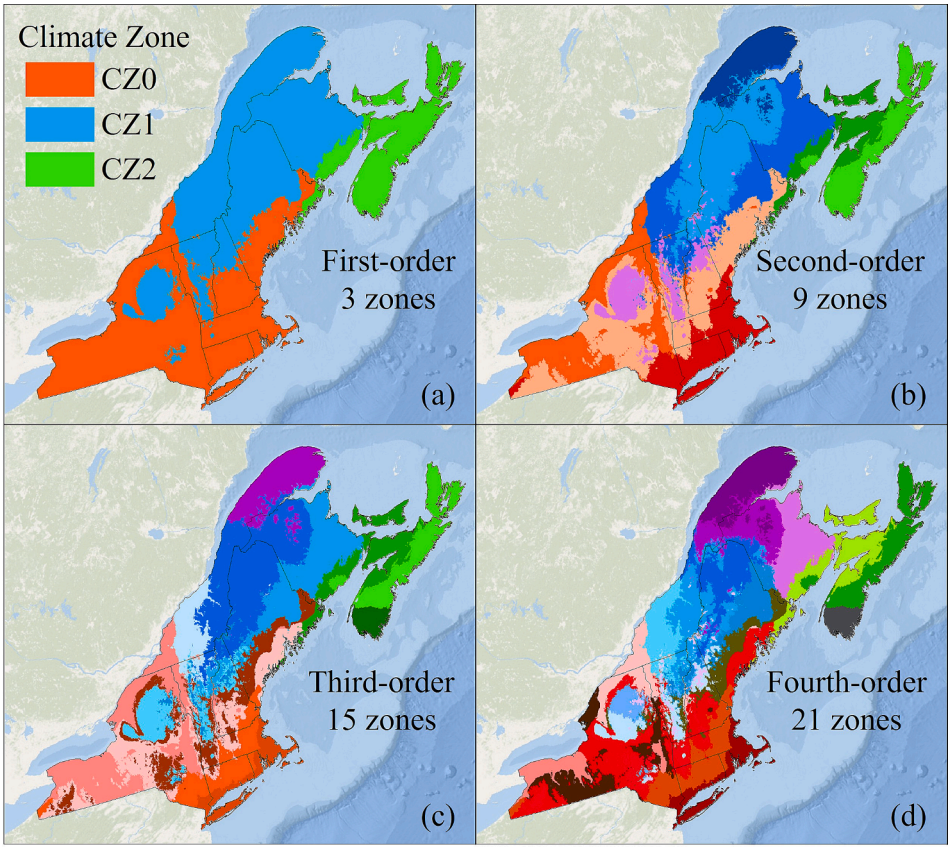

Fig. 4. The climate zones in the northeastern United States and maritime Canada are delineated into four orders based on the climate normals from 1961 to 1990, featuring increasing subzone resolutions of 3 (a), 9 (b), 15 (c), and 21 (d).

(Fig. 3a). CZ2 is characterized by the highest precipitation and mean annual relative humidity (Fig. 4b and 4d). In addition, it has moderate levels of mean annual temperature (Fig. 4a) and the fewest frost-free days (Fig. 4c), is distinct from the other two climate zones.

To explore second-order zones, we defined 9 climate zones and segmented CZ0 into three, CZ1 into four, and CZ2 into two subzones (Fig. 5b). When we increased the resolution to 15 climate zones to examine third-order zones, CZ0 was divided into six third-order zones, CZ1 into six, and CZ2 into three (Fig. 5c). To achieve even higher resolution, we defined 21 climate zones to generate fourth-order zones, resulting in CZ0 being divided into eight, CZ1 into ten, and CZ2 into three subzones (Fig. 5d). By increasing the level of classification, our approach was able to provide more detailed information about the climate zones and their boundaries.

3.2. Elevation-based comparison of climate zones

Elevation plays a pivotal role in shaping the spatial patterns of climate zones due to its profound influence on temperature, precipitation, and atmospheric pressure (Beniston et al., 1997; Lloyd, 2005; Rangwala and Miller, 2012). To compare our climate zone delineation, we examined the correlation between the first-order of climate zones and the elevation within our study area. The three first-order climate zones exhibit significant variations in their average elevations, underscoring their distinctness. CZ1 has the highest average elevation at 317 ± 190 m, while CZ2 features the lowest at 104 ± 89 m, and CZ0 displays an average elevation of 227 ± 169 m (Fig. 6). This disparity in elevation is a crucial factor in determining the spatial pattern of these climate zones, as higher elevations generally exhibit cooler temperatures and distinct weather patterns such as the Adirondack Mountains and Appalachian Mountains.

3.3. Climate zone shifts

Using the cluster parameters established for delineating the historic climate data from 1960 to 1990, we characterized the shift of each first-order climate zone under both SSP2-4.5 and SSP5-8.5 climate change scenarios (Fig. 7). Our findings indicate that CZ0 is anticipated to experience a consistent increase, expanding from 40 % coverage of the study region during the period of 1961–1990 to 89 % coverage between 2071 and 2100 under the SSP2-4.5 scenario (Fig. 7). Meanwhile, CZ1 and CZ2 are projected to decline from 46 % and 14 % coverage, respectively, to 8 % and 3 % coverage during the same time frame (Fig. 7). In contrast, under the more extreme SSP5-8.5 scenario, CZ0 is expected to almost dominate the entire region, leaving CZ1 to vanish completely and CZ2 to be conserved by a few isolated hotspots at the peaks of mountains (Fig. 7).

3.4. Forest ecosystem changes

CZ0, CZ1, and CZ2 represent distinct climate zones (CZs), each characterized by unique forest types (Fig. 8). CZ0 is predominantly composed of temperate broadleaf forests (Fig. 8a), with a moderate forest age of 87 ± 9 years (Fig. 8b and 9) and the highest canopy height in the study, measuring 16 ± 15 m (Fig. 8c and 9). Conversely, CZ2 is marked by greater complexity, encompassing both temperate broadleaf and mixed forests. This zone is characterized by the youngest forests, with an average age of 78 ± 9 years, and the lowest canopy height at 13 ± 10 m. CZ1, primarily consisting of mixed forests and temperate needleleaf forests, acts as an ecotone, bridging temperate broadleaf and needleleaf forests. It features an average canopy height of 14 ± 11 m and contains the oldest forests in the study, with an average age of 103 ± 11 years.

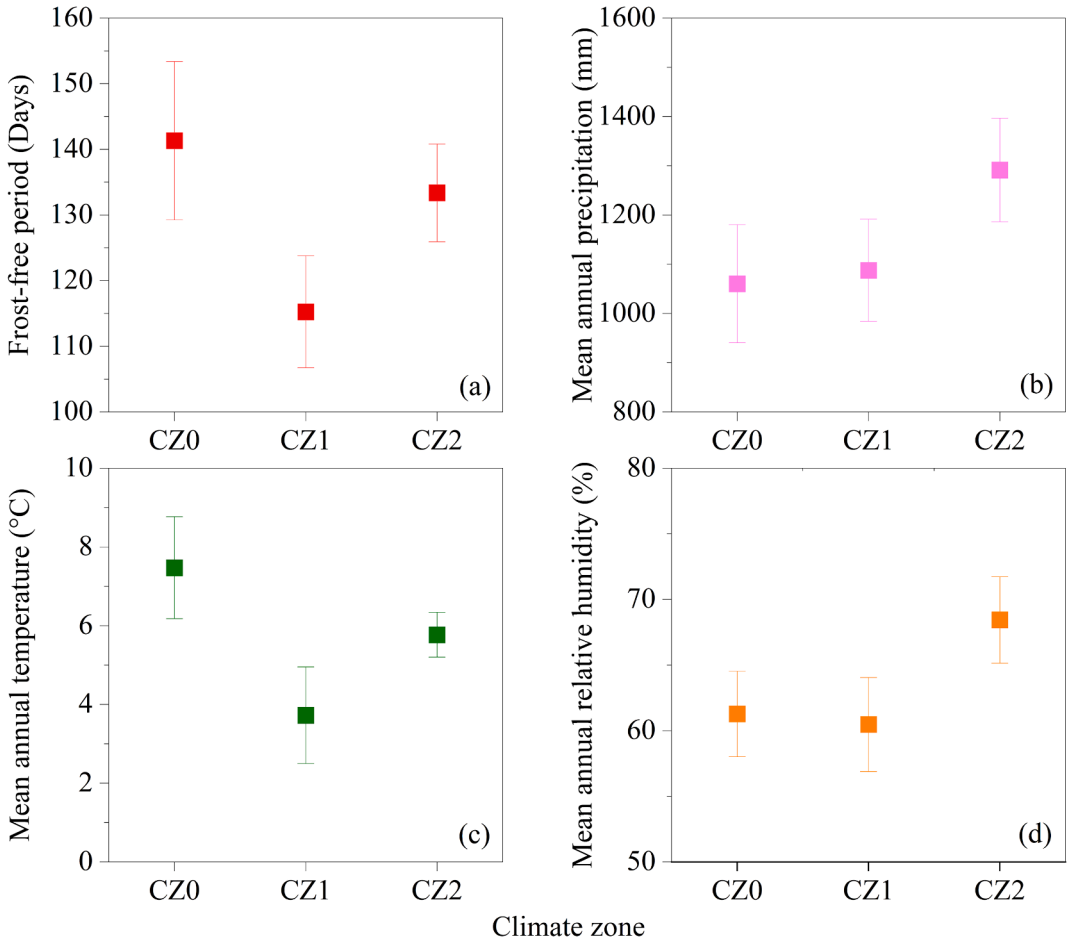

Fig. 5. The four major climate variables: forest-free period (a), mean annual precipitation (b), mean annual temperature (c), and mean annual relative humidity (d) for the three first-order climate zones delineated by using climate normals during the period of 1960–1990.

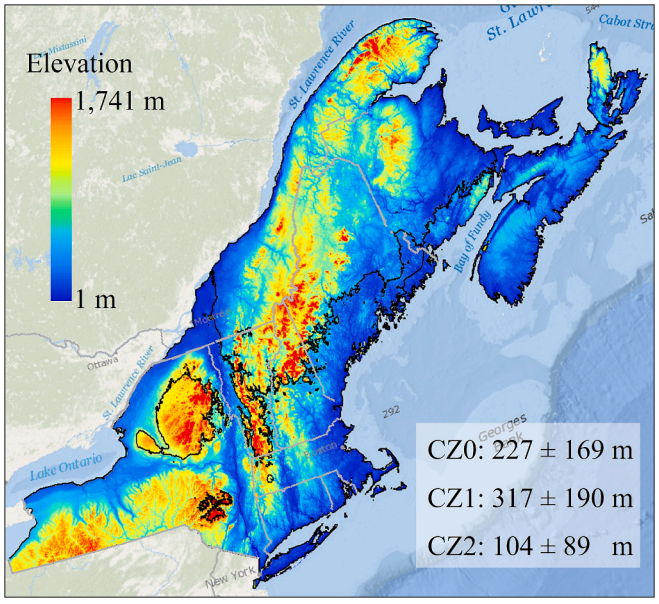

Fig. 6. The elevation spatial patterns of the northeastern United States and maritime Canada and average elevation for each climate zone, overlaid with the first-order climate zone boundary.

In terms of Aboveground Biomass (AGB) density (Fig. 8d and 9), CZ1 exhibits an average of 480 ± 240 MgC/ha, a reflection of its complex forest structure and age. CZ0 has an AGB density averaging 453 ± 315 MgC/ha. In contrast, CZ2 presents the lowest average AGB density at 351 ± 203 MgC/ha. At the forth level of delineated climate zones, forest matrix including the forest age, canopy height, and AGB are significantly different across these climate zones (Fig. 9), which indicates that the climate zone can significantly shape the forest ecosystems. At the fourth level of delineated climate zones, significant differences are observed in forest matrix such as forest age, canopy height, and AGB across these zones (Fig. 9). This suggests that the climate zone significantly influences the characteristics of forest ecosystems.

Anticipated climate changes are expected to reduce the areas of CZ1 and CZ2, currently comprising 46 % and 14 % of the study area, respectively. This will likely lead to an increased dominance of CZ0 in the region. Such a shift is projected to result in younger forest ages, higher canopies, and a decrease in carbon storage within the study area. Understanding these shifts in climate zones is crucial for predicting changes in forest ecosystems. In addition, the FIA plots with stand ages over 100 years indicate that CZ1 has an average AGB density of 1016 ± 291 MgC/ha. CZ0 has an average AGB density of 908 ± 297 MgC/ha. In contrast, CZ2 presents the lowest average AGB density at 859 ± 306 MgC/ha. These forest plots, being over a century old, exhibit AGB densities significantly higher than those derived from remote sensing images. Nonetheless, both data sets suggest that higher temperatures and lower precipitation can reduce forest carbon storage.

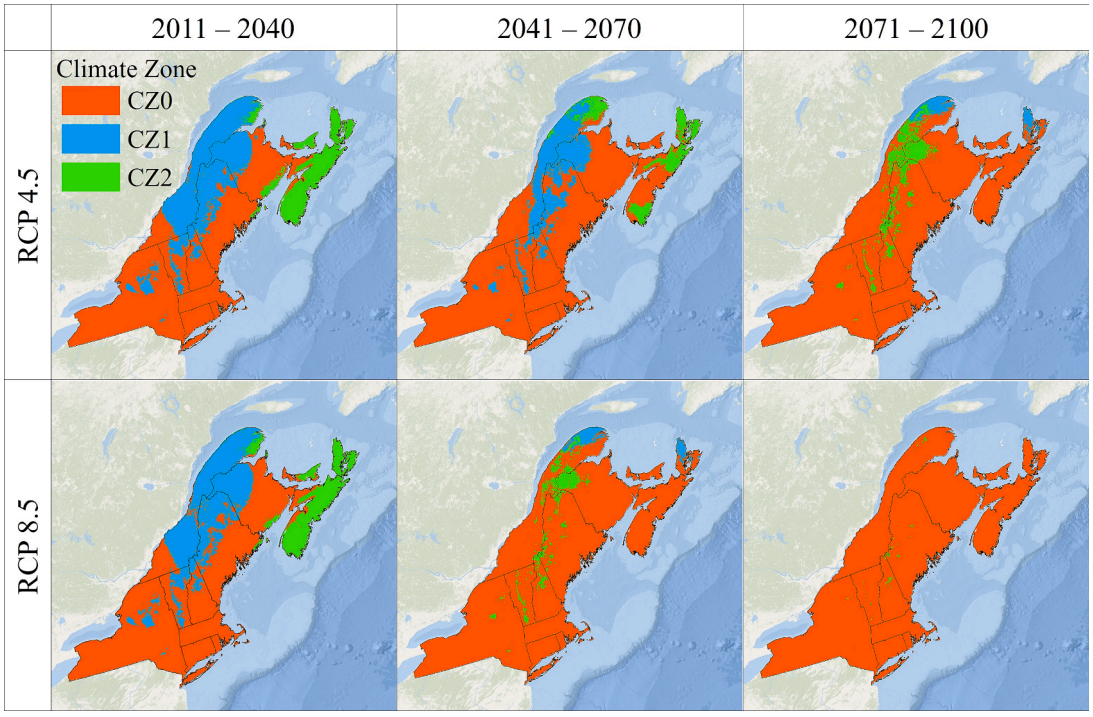

Fig. 7. Climate zones delineated by using predicted climate normals for the three periods of 2011–2040, 2041–2070, and 2071–2100 under SSP2-4.5 and SSP5-8.5 scenarios.

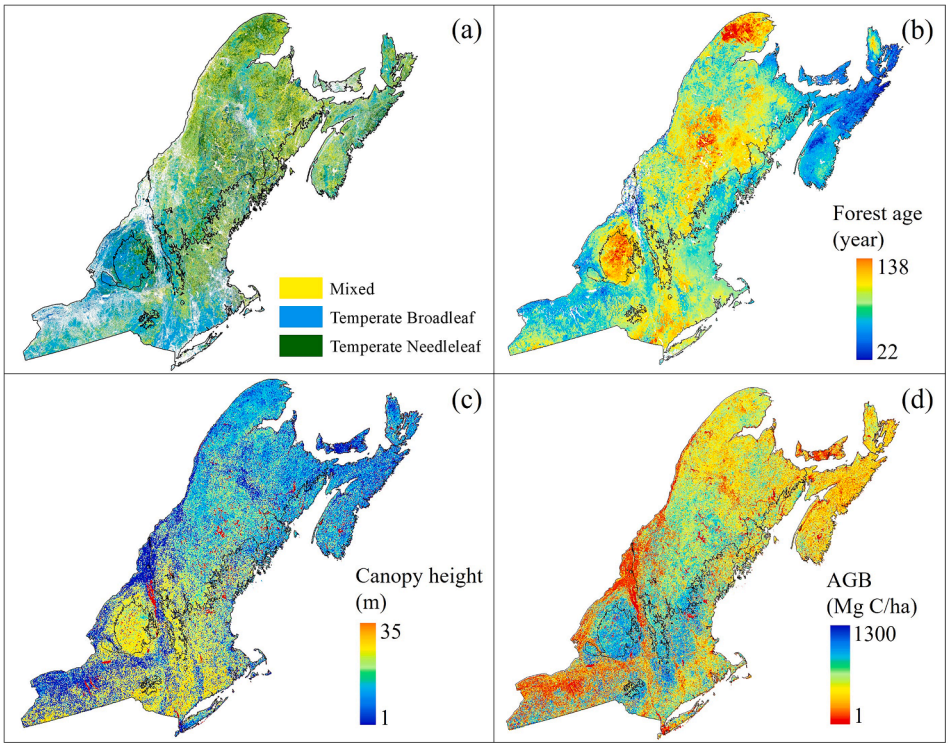

Fig. 8. The forest type (a), forest age (b), canopy height (c), and the aboveground biomass (AGB) density (d) for the entire study area, overlaid with the first-order climate zones.

4. Discussion

This proposed approach efficiently delineates climate zones and projects their shifts in the northeastern United States and maritime Canada, and it has advantages in five key aspects. First, this approach uses finer resolution (1 × 1 km) climate data to delineate climate regions. The finer spatial resolution climate data leads to more precise climate zone delineation, and the abundant climate variables provide a more comprehensive description of climate conditions. Second, PCA is included in this approach to reduce climate data dimensionality,

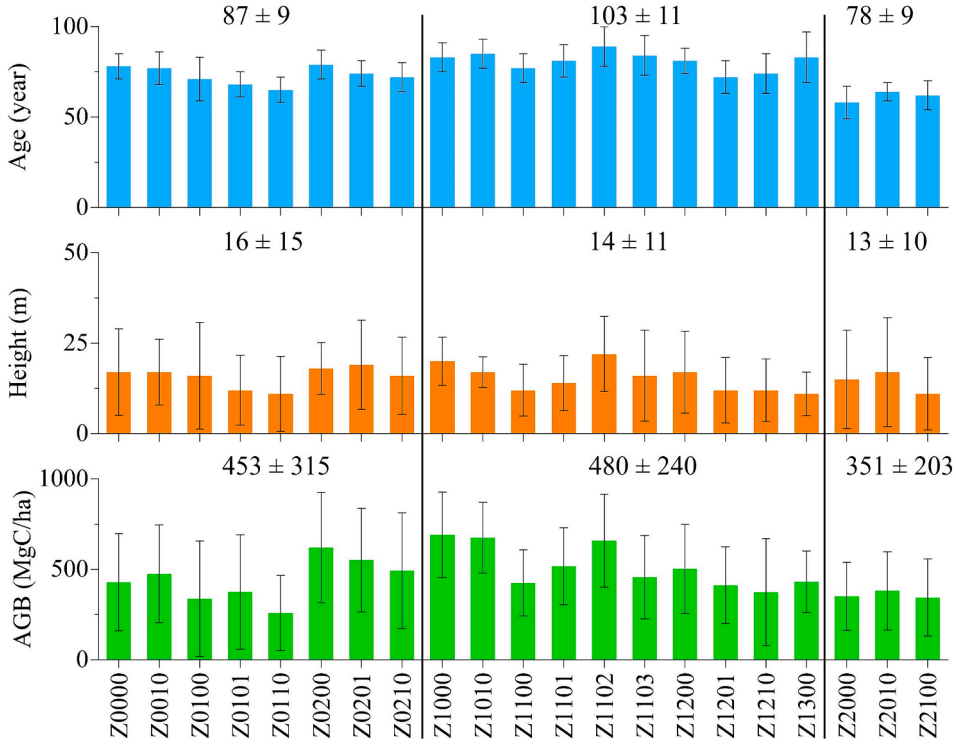

Fig. 9. The average forest age, canopy height, and aboveground biomass (AGB) for each forth-order climate zone. The climate zone number is a four-digit code where each digit represents a climate zone order: the first digit is for the first-order, the second for the second-order, the third for the third-order, and the fourth for the fourth-order.

improve interpretation, and overcome overfitting issues. By identifying highly correlated climate variables, this approach can effectively capture the dominant climate variables and thus make the delineation more efficient. Third, a group of samples is selected, clusters are generated initially using an agglomerative algorithm, and then a *K*-nearest neighbor classification algorithm is used to delineate each climate zone. This can considerably decrease computational time, enabling climate zone delineation for national, continental, and global regions. Fourth, the silhouette score is introduced to identify the optimal sampling strategy and the number of climate zones, reducing uncertainties associated with sample selection. Fifth, the local outlier factor algorithm is used to identify regions with significant climate change and regroup them. This approach clearly illustrates the changes and shifts within each climate zone under various future climate scenarios.

However, this approach delineates future climate zones by clustering historical climate normals, inherently assuming that future climates will mirror those within the historical record. While this methodology effectively utilizes existing climate data to predict shifts, it may not fully capture the emergence of novel climate conditions without historical precedents in the region. This limitation may overlook non-climatic analogues of future climate characteristics, potentially leading to significant alterations in the spatial distribution and traits of climate zones. The reliance on historical climate data as the foundation for future projections can shape our predictions, suggesting a degree of caution in extrapolating these findings to future scenarios. Thus, integrating more dynamic models that can account for the possibility of unprecedented climate conditions would improve the robustness and relevance of our projections, thereby enhancing our understanding of and response to the impacts of climate change on forest ecosystems.

These climate zone delineation findings highlight that the northeastern United States and maritime Canada encompass a diverse array of climate zones (Fig. 4). However, with the ongoing rapid climate warming, the diversity of climate zones is anticipated to decrease (Fig. 7), leading to CZ0 emerging as the dominant zone across the entire region. The proposed approach delineates higher-order climate zones based on the characteristics of the first-order climate zones. As a result, enhancing the homogeneity of the first-order climate zones leads to a reduction in the overall number of higher-order climate zones. Climate zone CZ0, characterized by high temperatures and low precipitation (Fig. 5), can profoundly impact tree species (Seddon et al., 2016), forest disturbances (Chen et al., 2019; Wei et al., 2018), and forest ecosystem productivity (Zhao et al., 2022b) in the study region. Therefore, delineating climate zones within this region and projecting their shifts is essential to guide the development of effective management and conservation strategies, ensuring long-term forest ecosystem sustainability.

Current research underscores the impact of climate change on forest ecosystems such as composition, structure, and disturbances (Liang et al., 2018; Liang et al., 2023). For instance, climate warming not only introduces conditions that favor warm-adapted tree species but also leads to the homogenization of tree species diversity (Boulanger et al., 2017). Our findings reveal that the climate zone characterized by warmer and drier conditions (CZ0) is expanding, poised to encompass the entire study region. This expansion is expected to modify the tree species composition in the other two zones, with temperate broadleaf forests becoming predominant. Forest inventory data from old-growth FIA plots within these zones indicate that temperate broadleaf forests in CZ0 exhibit a lower carbon storage capacity than those in CZ1. This suggests that shifts in climate zones may lead to a reduction in carbon storage within CZ1. Conversely, CZ2 currently has the lowest carbon storage capacity but may experience an increase due to these shifts, primarily driven by changes in tree species composition (Pérez-Cruzado et al., 2012).

Furthermore, the shift in climate zones towards warmer and drier conditions is likely to increase the frequency of disturbances such as insect outbreaks, droughts, and fires, further impacting forest ecosystems (Seidl et al., 2017). Consistent with our observations, forests in CZ0 tend to have younger trees, a factor that could diminish the carbon storage and timber productivity (Law et al., 2001; Zhao et al., 2022a).

This highlights the need for adaptive management and conservation strategies to mitigate the impacts of these disturbances (Zhao et al., 2023a). Understanding the complex relationship between climate zones and forest ecosystems allows for the development of management practices that enhance forest resilience, promote species diversity, and ensure the sustainability of these essential natural resources in the face of climate change (Keenan, 2015).

5. Conclusions

The methodology introduced for delineating climate zones offers a robust framework for understanding existing climate patterns and forecasting their evolution under different future climate scenarios. Grasping these climate zone shifts is vital for anticipating alterations in forest ecosystems. In the northeastern United States and maritime Canada, the climate zones we have identified play a pivotal role in pinpointing forest ecosystems with significant conservation value and informing policy decisions. Moreover, our projections suggest a movement towards more homogeneous climate zones across the region. This trend is expected to result in forests with younger ages, taller canopies, and reduced carbon storage capabilities. Such insights underscore the necessity for adaptive management and conservation strategies to mitigate the impacts of climate change on forest ecosystems, ensuring their resilience and sustainability for the future.

CRediT authorship contribution statement

Samuel Roy: Writing – original draft, Methodology, Formal analysis, Data curation, Conceptualization. **Xinyuan Wei:** Writing – review & editing, Writing – original draft, Visualization, Methodology, Formal analysis. **Aaron Weiskittel:** Writing – review & editing, Supervision, Funding acquisition, Conceptualization. **Daniel J. Hayes:** Writing – review & editing, Supervision, Funding acquisition. **Peter Nelson:** Writing – review & editing. **Alexandra R. Contosta:** Writing – review & editing.

Declaration of competing interest

The authors declare that they have no known competing financial interests or personal relationships that could have appeared to influence the work reported in this paper.

Data availability

I have shared the data link in the Data Availability Statement.

Acknowledgements

This project was supported by the National Science Foundation RII Track-2 FEC grant (# 1920908), USDA NIFA Sustainable Agricultural Systems grant (#2023-68012-38992), and the NASA Carbon Monitoring System grant (# 80NSSC21K0966).

Author Contribution Statement.

Samuel Roy and Aaron Weiskittel conceptualized and designed this project. Samuel Roy developed the climate zones delineation approach and applied it to delineate climate zones in northeastern United States and maritime Canada. Samuel Roy and Xinyuan Wei interpreted the results and wrote the original manuscript. Aaron Weiskittel and Daniel J. Hayes supervised the project. All authors contributed to the editing of the manuscript.

Data Availability Statement

All Python scripts used in this article can be found in https://github.com/xinyuanwylb19/ClimateZone. The delineated climate zones data and all data used to generate figures in this article can be found in https://github.com/xinyuanwylb19/ClimateZone. The climate data is derived from ClimateNA (accessed on April 1, 2022, https://climatena.ca/). The elevation data is obtained from United States Geological Survey (USGS, accessed on March 31, https://www.sciencebase.gov/catalog/item/4fb5495ee4b04cb937751d6d). The land cover data for the North America is obtained from the National Land Cover Database (NLCD, accessed on March 15, 2023, https://www.mrlc.gov/data/north-american-land-change-monitoring-system).

Appendix A. Supplementary data

Supplementary data to this article can be found online at https://doi.org/10.1016/j.ecolind.2024.111921.

References

Araújo, M.B., Alagador, D., Cabeza, M., Nogués-Bravo, D., Thuiller, W., 2011. Climate change threatens European conservation areas. Ecol. Lett. 14 (5), 484–492.
Atzberger, C., 2013. Advances in remote sensing of agriculture: context description, existing operational monitoring systems and major information needs. Remote Sens. (Basel) 5 (2), 949–981.
Beck, H.E., et al., 2018. Present and future köppen-Geiger climate classification maps at 1-km resolution. Sci. Data 5 (1), 1–12.
Beniston, M., Diaz, H., Bradley, R., 1997. Climatic change at high elevation sites: an overview. Clim. Change 36 (3–4), 233–251.
Besnard, S., et al., 2021. Mapping global forest age from forest inventories, biomass and climate data. Earth Syst. Sci. Data 13 (10), 4881–4896.
Boulanger, Y., et al., 2017. Climate change impacts on forest landscapes along the Canadian southern boreal forest transition zone. Landsc. Ecol. 32, 1415–1431.
Bramer, I., et al., 2018. Advances in monitoring and modelling climate at ecologically relevant scales. Adv. Ecol. Res. Elsevier 101–161.
Briggs, R., Lemin, R., 1992. Delineation of climatic regions in Maine. Can. J. For. Res. 22 (6), 801–811.
Bunkers, M.J., Miller, J.R., DeGaetano, A.T., 1996. Definition of climate regions in the Northern Plains using an objective cluster modification technique. J. Clim. 9 (1), 130–146.
Chapin, F.S., et al., 2006. Reconciling carbon-cycle concepts, terminology, and methods. Ecosystems 9 (7), 1041–1050.
Chen, C., Wei, X., Weiskittel, A., Hayes, D.J., 2019. Above-ground carbon stock in merchantable trees not reduced between cycles of spruce budworm outbreaks due to changing species composition in spruce-fir forests of Maine, USA. For. Ecol. Manage. 453, 117590.
Chomboon, K., Chujai, P., Teerarassamee, P., Kerdprasop, K., Kerdprasop, N., 2015. An empirical study of distance metrics for k-nearest neighbor algorithm. Proceedings of the 3rd International Conference on Industrial Application Engineering.
Daffertshofer, A., Lamoth, C.J., Meijer, O.G., Beek, P.J., 2004. PCA in studying coordination and variability: a tutorial. Clin. Biomech. 19 (4), 415–428.
Dalmaijer, E.S., Nord, C.L., Astle, D.E., 2022. Statistical power for cluster analysis. BMC Bioinf. 23 (1), 1–28.
Danneyrolles, V., et al., 2019. Stronger influence of anthropogenic disturbance than climate change on century-scale compositional changes in northern forests. Nat. Commun. 10 (1), 1265.
de Sá Júnior, A., de Carvalho, L.G., Da Silva, F.F., de Carvalho Alves, M., 2012. Application of the köppen classification for climatic zoning in the state of Minas Gerais, Brazil. Theor. Appl. Climatol. 108, 1–7.
Demuzere, M., Bechtel, B., Mills, G., 2019. Global transferability of local climate zone models. Urban Clim. 27, 46–63.
Evans, P., Brown, C.D., 2017. The boreal–temperate forest ecotone response to climate change. Environ. Rev. 25 (4), 423–431.
Fernandez, I.J. et al., 2020. Maine's climate future: 2020 update.
Formann, A.K., 1984. Die latent-class-analyse: Einführung in Theorie und Anwendung. Beltz.
Freeman, B.G., Song, Y., Feeley, K.J., Zhu, K., 2021. Montane species track rising temperatures better in the tropics than in the temperate zone. Ecol. Lett. 24 (8), 1697–1708.
Fujisawa, H., Eguchi, S., 2008. Robust parameter estimation with a small bias against heavy contamination. J. Multivar. Anal. 99 (9), 2053–2081.
Gardner, A.S., Maclean, I.M., Gaston, K.J., 2020. A new system to classify global climate zones based on plant physiology and using high temporal resolution climate data. J. Biogeogr. 47 (10), 2091–2101.
Geletič, J., Lehnert, M., Dobrovolný, P., Žuvela-Aloise, M., 2019. Spatial modelling of summer climate indices based on local climate zones: expected changes in the future climate of Brno, Czech Republic. Clim. Change 152, 487–502.
Gilliam, F.S., 2016. Forest ecosystems of temperate climatic regions: from ancient use to climate change. New Phytol. 212 (4), 871–887.
Gounand, I., Little, C.J., Harvey, E., Altermatt, F., 2020. Global quantitative synthesis of ecosystem functioning across climatic zones and ecosystem types. Glob. Ecol. Biogeogr. 29 (7), 1139–1176.
Grimm, N.B., et al., 2013. The impacts of climate change on ecosystem structure and function. Front. Ecol. Environ. 11 (9), 474–482.
Gullett, D. and Skinner, W.R., 1992. The state of Canada's climate: temperature change in Canada 1895-1991.
Habel, J.C., et al., 2019. Final countdown for biodiversity hotspots. Conserv. Lett. 12 (6), e12668.

Hoffmann, A., et al., 2015. A framework for incorporating evolutionary genomics into biodiversity conservation and management. Climate Change Responses 2, 1–24.
Iyigun, C., et al., 2013. Clustering current climate regions of Turkey by using a multivariate statistical method. Theor. Appl. Climatol. 114, 95–106.
Keenan, R.J., 2015. Climate change impacts and adaptation in forest management: a review. Ann. For. Sci. 72, 145–167.
Laganiere, J., Angers, D.A., Pare, D., 2010. Carbon accumulation in agricultural soils after afforestation: a meta-analysis. Glob. Chang. Biol. 16 (1), 439–453.
Law, B., Thornton, P., Irvine, J., Anthoni, P., Van Tuyl, S., 2001. Carbon storage and fluxes in ponderosa pine forests at different developmental stages. Glob. Chang. Biol. 7 (7), 755–777.
Leduc, M., et al., 2019. The ClimEx project: A 50-member ensemble of climate change projections at 12-km resolution over Europe and northeastern North America with the Canadian regional climate model (CRCM5). J. Appl. Meteorol. Climatol. 58 (4), 663–693.
Liang, Y., et al., 2023. What is the role of disturbance in catalyzing spatial shifts in forest composition and tree species biomass under climate change? Glob. Chang. Biol. 29 (4), 1160–1177.
Liang, Y., Duveneck, M.J., Gustafson, E.J., Serra-Diaz, J.M., Thompson, J.R., 2018. How disturbance, competition, and dispersal interact to prevent tree range boundaries from keeping pace with climate change. Glob. Chang. Biol. 24 (1), e335–e351.
Liu, S., Shi, Q., 2020. Local climate zone mapping as remote sensing scene classification using deep learning: a case study of metropolitan China. ISPRS J. Photogramm. Remote Sens. 164, 229–242.
Lloyd, C., 2005. Assessing the effect of integrating elevation data into the estimation of monthly precipitation in Great Britain. J. Hydrol. 308 (1–4), 128–150.
Mahmud, S., Sumana, F.M., Mohsin, M., Khan, M.H.R., 2022. Redefining homogeneous climate regions in Bangladesh using multivariate clustering approaches. Nat. Hazards 111 (2), 1863–1884.
Mahony, C.R., Wang, T., Hamann, A., Cannon, A.J., 2022. A global climate model ensemble for downscaled monthly climate normals over North America. Int. J. Climatol. 42 (11), 5871–5891.
Manes, S., et al., 2021. Endemism increases species' climate change risk in areas of global biodiversity importance. Biol. Conserv. 257, 109070.
Mishra, S. and Chawla, M., 2019. A comparative study of local outlier factor algorithms for outliers detection in data streams, Emerging Technologies in Data Mining and Information Security: Proceedings of IEMIS 2018, Volume 2. Springer, pp. 347-356.
Murtagh, F., Legendre, P., 2014. Ward's hierarchical agglomerative clustering method: which algorithms implement Ward's criterion? J. Classif. 31, 274–295.
NCEI, 2023. NOAA, National Centers for Environmental Information, Climate Data Record (CDR).
Nusrat, A., et al., 2020. Application of machine learning techniques to delineate homogeneous climate zones in river basins of Pakistan for hydro-climatic change impact studies. Appl. Sci. 10 (19), 6878.
Oldfather, M.F., Kling, M.M., Sheth, S.N., Emery, N.C., Ackerly, D.D., 2020. Range edges in heterogeneous landscapes: integrating geographic scale and climate complexity into range dynamics. Glob. Chang. Biol. 26 (3), 1055–1067.
Pérez-Cruzado, C., Mansilla-Salinero, P., Rodríguez-Soalleiro, R., Merino, A., 2012. Influence of tree species on carbon sequestration in afforested pastures in a humid temperate region. Plant Soil 353, 333–353.
Potapov, P., et al., 2021. Mapping global forest canopy height through integration of GEDI and landsat data. Remote Sens. Environ. 253, 112165.
Qiu, W. and Joe, H., 2009. clusterGeneration: random cluster generation (with specified degree of separation). R package version, 1(7): 75275-0122.
Rahbek, C., et al., 2019. Humboldt's enigma: what causes global patterns of mountain biodiversity? Science 365 (6458), 1108–1113.
Rangwala, I., Miller, J.R., 2012. Climate change in mountains: a review of elevation-dependent warming and its possible causes. Clim. Change 114, 527–547.
Rhee, J., Im, J., Carbone, G.J., Jensen, J.R., 2008. Delineation of climate regions using in-situ and remotely-sensed data for the Carolinas. Remote Sens. Environ. 112 (6), 3099–3111.
Ricketts, T.H., 1999. Terrestrial ecoregions of North America: a conservation assessment, 1. Island Press.
Rosentreter, J., Hagensieker, R., Waske, B., 2020. Towards large-scale mapping of local climate zones using multitemporal sentinel 2 data and convolutional neural networks. Remote Sens. Environ. 237, 111472.
Samal, N.R., et al., 2017. A coupled terrestrial and aquatic biogeophysical model of the upper Merrimack River watershed, New Hampshire, to inform ecosystem services evaluation and management under climate and land-cover change. Ecol. Soc. 22 (4).
Seddon, A.W., Macias-Fauria, M., Long, P.R., Benz, D., Willis, K.J., 2016. Sensitivity of global terrestrial ecosystems to climate variability. Nature 531 (7593), 229–232.
Seidl, R., et al., 2017. Forest disturbances under climate change. Nat. Clim. Chang. 7 (6), 395–402.
Shahapure, K.R., Nicholas, C., 2020. Cluster quality analysis using silhouette score, 2020 IEEE 7th international conference on data science and advanced analytics (DSAA). IEEE 747–748.
Spawn, S., Gibbs, H., 2020. Global aboveground and belowground biomass carbon density maps for the year 2010. Ornl Daac.
Szekely, G.J., Rizzo, M.L., 2005. Hierarchical clustering via joint between-within distances: extending Ward's minimum variance method. J. Classif. 22 (2), 151–184.
Taheri, S., Naimi, B., Rahbek, C., Araújo, M.B., 2021. Improvements in reports of species redistribution under climate change are required. Sci. Adv. 7 (15), eabe1110.
Trew, B.T., Maclean, I.M., 2021. Vulnerability of global biodiversity hotspots to climate change. Glob. Ecol. Biogeogr. 30 (4), 768–783.
von Buttlar, J., et al., 2018. Impacts of droughts and extreme-temperature events on gross primary production and ecosystem respiration: a systematic assessment across ecosystems and climate zones. Biogeosciences 15 (5), 1293–1318.
Walther, G.-R., et al., 2002. Ecological responses to recent climate change. Nature 416 (6879), 389–395.
Wang, T., Hamann, A., Spittlehouse, D., Carroll, C., 2016. Locally downscaled and spatially customizable climate data for historical and future periods for North America. PLoS One 11 (6), e0156720.
Wei, X., Hayes, D.J., Fraver, S., Chen, G., 2018. Global pyrogenic Carbon production during recent decades has created the potential for a Large, long-term sink of atmospheric CO2. J. Geophys. Res. Biogeo. 123 (12), 3682–3696.
Wei, X., Hayes, D.J., Li, D., Butman, D.E., Brewin, R.J., 2024. Fates of terrigenous dissolved organic Carbon in the Gulf of Maine. Environ. Sci. Tech.
Xu, H., Zhang, L., Li, P., Zhu, F., 2022. Outlier detection algorithm based on k-nearest neighbors-local outlier factor. J. Algorith. Computat. Technol. 16, 17483026221078111.
Yang, L., et al., 2018. A new generation of the United States National Land Cover Database: requirements, research priorities, design, and implementation strategies. ISPRS J. Photogramm. Remote Sens. 146, 108–123.
Zhao, J., et al., 2023b. Exploring plausible contributions of end-use harvested wood products to store atmospheric carbon in China. Biomass Bioenergy 177, 106934.
Zhao, J., Daigneault, A., Weiskittel, A., 2022a. Estimating regional timber supply and forest carbon sequestration under shared socioeconomic pathways: a case study of Maine, USA. PLOS Climate 1 (5), e0000018.
Zhao, J., Wei, X., Li, L., 2022b. The potential for storing carbon by harvested wood products. Front Forest. Global Change 238.
Zhao, J., Daigneault, A., Weiskittel, A., Wei, X., 2023a. Climate and socioeconomic impacts on Maine's forests under alternative future pathways. Ecol. Econ. 214, 107979.
Zheng, C., Wu, J., Zhai, X., Wang, R., 2016. Impacts of feed-in tariff policies on design and performance of CCHP system in different climate zones. Appl. Energy 175, 168–179.